RNA (2001), *7*:702–709. Cambridge University Press. Printed in the USA.

The *Escherichia coli* DEAD protein DbpA recognizes a small RNA hairpin in 23S rRNA

CHRISTOPHER A. TSU,[1] KARL KOSSEN, and OLKE C. UHLENBECK
Department of Chemistry and Biochemistry, University of Colorado, Boulder, Colorado 80309-0215, USA

ABSTRACT

The *Escherichia coli* DEAD protein DbpA is an RNA-specific ATPase that is activated by a 153-nt fragment within domain V of 23S rRNA. A series of RNA subfragments and sequence changes were used to identify the recognition elements of this RNA–protein interaction. Reducing the size of the fully active 153-nt RNA yields compromised substrates in which both RNA and ATP binding are weakened considerably without affecting the maximal rate of ATP hydrolysis. All RNAs that stimulate ATPase activity contain hairpin 92 of 23S rRNA, which is known to interact with the 3′ end of tRNAs in the ribosomal A-site. RNAs with base mutations within this hairpin fail to activate ATP hydrolysis, suggesting that it is a critical recognition element for DbpA. Although the isolated hairpin fails to activate DbpA, RNAs with an extension of approximately 15 nt on either the 5′ or 3′ side of hairpin 92 elicit full ATPase activity. These results suggest that the binding of DbpA to RNA requires sequence-specific interactions with hairpin 92 as well as nonspecific interactions with the RNA extension. A model relating the RNA binding and ATPase activities of DbpA is presented.

Keywords: ATPase; DEAD protein; RNA–protein interaction; rRNA

INTRODUCTION

Members of the DEAD, DEAH, and DExH (collectively $DEx^D/_H$) protein families are involved in many facets of RNA metabolism, including translation initiation, ribosome biogenesis, pre-mRNA splicing, and mRNA degradation (Wassarman & Steitz, 1991; Schmid & Linder, 1992; Pause & Sonenberg, 1993; Anderson & Parker, 1996; de la Cruz et al., 1999). The $DEx^D/_H$ proteins are members of the second of three loosely related helicase superfamilies, the first two of which show considerable structural similarity within the two domains that contain the conserved sequence motifs (Korolev et al., 1998). $DEx^D/_H$ proteins typically display an RNA-dependent ATPase activity, and several have been shown to possess an ATP-dependent RNA helicase activity in vitro (Hirling et al., 1989; Pause & Sonenberg, 1992; Preugschat et al., 1996; Laggerbauer et al., 1998; Wang et al., 1998; Rogers et al., 1999; Jankowsky et al., 2000). Because several $DEx^D/_H$ proteins participate in processes in which stable RNA structures are disrupted or rearranged, it is widely believed that $DEx^D/_H$ proteins facilitate RNA isomerizations (Fuller-Pace, 1994; Luking et al., 1998; Staley & Guthrie, 1998).

DbpA is the founding member of a subfamily of bacterial DEAD proteins that are specifically activated by a region of domain V of 23S ribosomal RNA (Tsu & Uhlenbeck, 1998; Kossen & Uhlenbeck, 1999; Pugh et al., 1999). Although most $DEx^D/_H$ proteins act on defined RNAs in vivo, this may be dependent on accessory proteins, as the purified proteins typically lack RNA specificity in vitro (Fuller-Pace, 1994; Staley & Guthrie, 1998). The unique RNA specificity of DbpA and its homologs appears to be associated with a highly conserved carboxy-terminal domain (Kossen & Uhlenbeck, 1999). A defined RNA specificity in the absence of accessory proteins makes DbpA an excellent system in which to study the molecular function and mechanism of DEAD proteins. Although DbpA's biological function is not known, its RNA target adopts a complex fold within the ribosome (Ban et al., 2000), suggesting a role for DbpA in translation or ribosome biogenesis.

A 153-nt fragment of 23S rRNA that fully stimulates the ATPase activity of DbpA was previously identified and used to examine several fundamental parameters including the stoichiometry of the RNA–protein complex and the energetic barriers to ATP hydrolysis (Fig. 1A; Nicol & Fuller-Pace, 1995; Tsu & Uhlenbeck,

Reprint requests to: Olke C. Uhlenbeck, Department of Chemistry and Biochemistry, Campus Box 215, University of Colorado, Boulder, Colorado 80309-0215, USA; e-mail: Olke.Uhlenbeck@Colorado.edu.
[1] Present address: Newborn Medicine, Children's Hospital, 300 Longwood Avenue, Enders 970, Boston, Massachusetts 02115-5737, USA; e-mail: christopher.tsu@TCH.Harvard.edu.

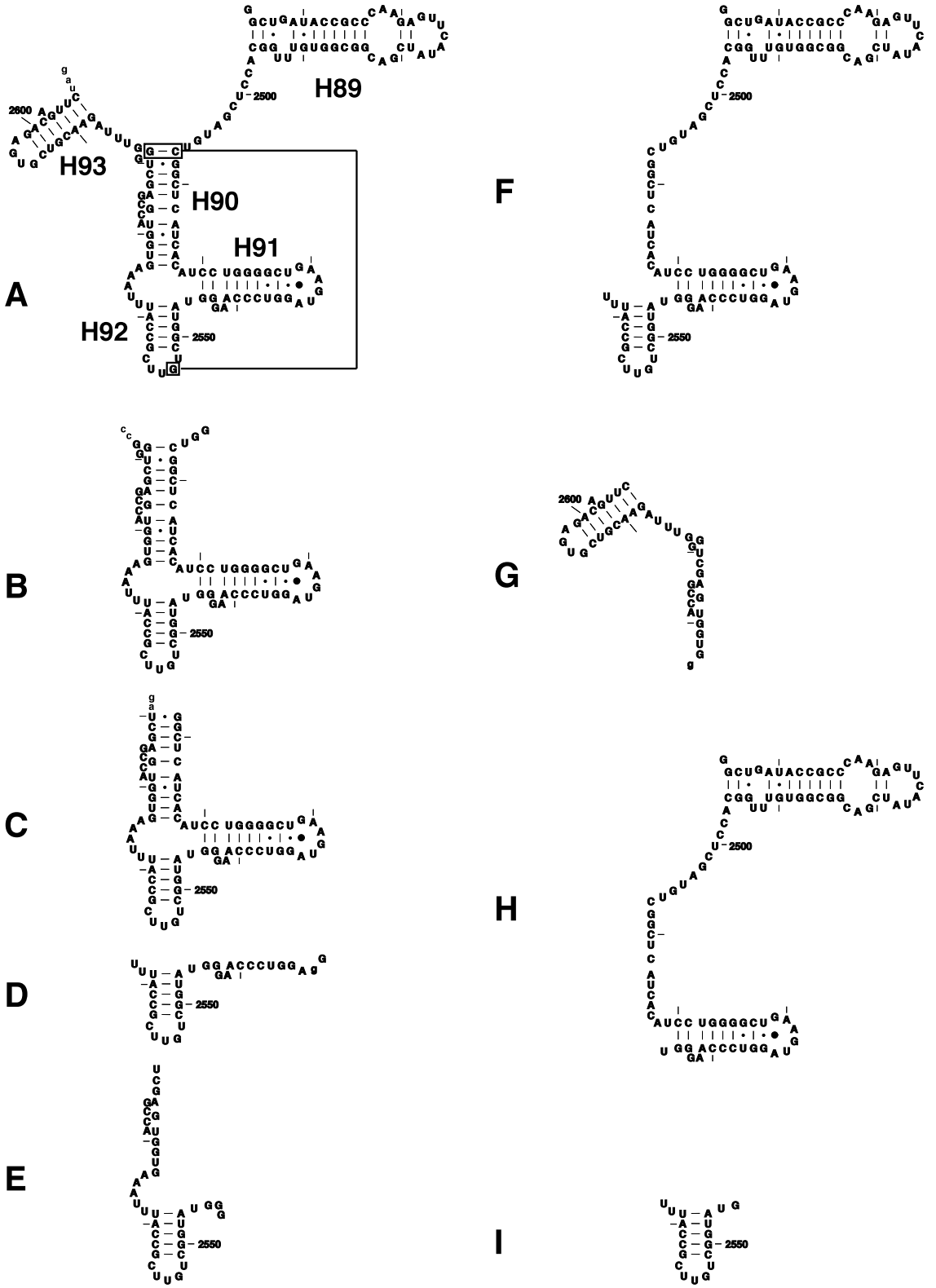

FIGURE 1. Fragments of *E. coli* 23S rRNA used in this work. For ease of comparison, secondary structures are presented in the format of 23S rRNA and are not intended to represent the structure of these RNAs in solution. Lowercase letters indicate residues that are present in transcripts that are not part of the 23S sequence. Helices 89 to 93 of 23S rRNA (Leffers et al., 1987) are indicated on cofactor A. The C2507-G2582 base pair forms a base triple with G2553 in the 50S subunit structure as indicated in RNA A (Ban et al., 2000). Secondary structures were obtained from The Comparative RNA Web Page at http://www.rna.icmb.utexas.edu/.

1998). Although this transcript lacks the posttranscriptional modifications found in rRNA, it is kinetically identical to the native, full-length 23S rRNA and presumably contains all the determinants of RNA-dependent ATPase activity. Here the size and sequence dependence of the DbpA-binding site are investigated using subfragments of the 153-nt RNA and sequence mutants. The results of this study indicate that DbpA specifically recognizes 23S hairpin 92; however additional interactions with a sequence nonspecific RNA extension are required to elicit ATPase activity. These results support a model in which the recognition of hairpin 92 by the unique carboxy-terminus of DbpA defines the sequence specificity of the protein, and additional contacts between the RNA backbone and the helicase domains contribute to the RNA-binding affinity and are required for RNA-dependent ATPase activity.

RESULTS AND DISCUSSION

Truncation of the DbpA binding site

A 153-nt transcript of *Escherichia coli* 23S rRNA (Fig. 1, RNA A) fully stimulates the ATPase activity of DbpA (Tsu & Uhlenbeck, 1998). To identify the elements within RNA A required for the stimulation of ATP hydrolysis, we analyzed the ability of eight subfragments of this RNA to activate DbpA (Fig. 1, fragments B–I). Although RNA clearly activates enzymatic ATP hydrolysis, any effect of DbpA on the RNA has yet to be identified. Therefore, the RNA was treated as a cofactor of the ATP hydrolysis reaction rather than a true substrate and the maximal catalytic rate (k_{max}) supported by each RNA and its apparent binding constant ($K_{app,RNA}$) were obtained by measuring the rate of ATP hydrolysis under conditions of saturating ATP and varying concentrations of RNA.

Table 1 lists k_{max} values for RNAs A–I that indicate that a given RNA either elicits a high rate of ATP hydrolysis (300–580 min^{-1}), or none at all. These results generally agree with the work of Fuller-Pace and coworkers, who observed that RNA C and a slightly larger 93-nt fragment promote ATPase activity (Nicol & Fuller-Pace, 1995; Pugh et al., 1999). Our results demonstrate that of the five helices predicted for cofactor A by phylogenetic sequence covariation (H89-93; Leffers et al., 1987), all activating RNAs contain hairpin 92. RNAs G and H, which lack hairpin 92, fail to activate ATP hydrolysis. Even a bimolecular complex of RNAs G and H, which reforms 85% of RNA A, fails to stimulate activity. Although all activating RNAs contain hairpin 92, it is striking that the isolated hairpin does not elicit detectable ATPase activity even at concentrations as high as 1 μM. Taken together, these results indicate that the RNA-dependent ATPase activity of DbpA requires hairpin 92 with either a 5′ or 3′ extension. These requirements cannot be fulfilled *in trans*, suggesting that the hairpin and RNA extension are bound cooperatively.

The apparent RNA-binding constants for RNAs A–F suggest that DbpA makes energetically important contacts throughout RNA A. RNA B, which lacks the 5′ and 3′ extensions of RNA A, shows a fourfold weaker $K_{app,RNA}$. Removing an additional seven residues from the top of helix 90 yields RNA C, and raises $K_{app,RNA}$ another ninefold. Further dissection of RNA C to yield RNAs D–F yields less than a further twofold increase in $K_{app,RNA}$. Assuming that $K_{app,RNA}$ values reflect the true RNA dissociation constant, the smaller RNAs D and E bind DbpA with approximately 80% of the free energy associated with RNA A. Nevertheless, the wide range of $K_{app,RNA}$ values for RNAs A–F despite very similar values of k_{max} suggests that there are additional RNA–protein interactions that contribute to RNA binding without affecting ATPase activity.

TABLE 1. Activity and kinetic constants of RNA fragments.

RNA	Nucleotides (*E. coli* 23S)	k_{max} (min^{-1})	$K_{app,RNA}$ (nM)	$k_{max}/K_{app,RNA}$ (min^{-1} nM^{-1})	k_{cat} (min^{-1})	$K_{M,ATP}$ (μM)	$k_{cat}/K_{M,ATP}$ (min^{-1} μM^{-1})
A	2454–2606	580[a]	11[a]	53	570[a]	120[a]	4.8
B	2504–2583	540	41	13	600	510	1.2
C	2508–2580	300	360	0.83	230	600	0.39
D	2532–2563	470	700	0.67	450	1000	0.45
E	2543–2580	410	660	0.63	240	650	0.37
F	2454–2563	430	430	1.0	490	180	2.7
G	2567–2606	—	—	≤0.002[b]	—	—	ND
H	2454–2546	—	—	≤0.002[b]	—	—	ND
I	2545–2563	—	—	≤0.002[b]	—	—	ND

Kinetic constants were determined in buffer A. The invariant substrate was held at saturating levels (5 mM ATP, or RNA concentrations at least sixfold over $K_{app,RNA}$). DbpA was in the range of 5–20 nM, and was less than the lowest substrate concentration used.

[a] Taken from Tsu and Uhlenbeck (1998).

[b] Estimated upper limit based on initial data.

The extensive nature of contacts between cofactor A and DbpA suggests that either the RNA-binding surface of DbpA is very large or that the RNA adopts a more compact structure. Although the structure of RNA A in solution is not known, the structure of this region in the 50S subunit is quite compact (Ban et al., 2000). In this structure, helices 90 and 91 are coaxially stacked, with helices 89 and 92 parallel and adjacent to them. Among the tertiary interactions that stabilize this region, nt 2553 of hairpin 92 forms a base triple with the C2507-G2582 base pair at the top of helix 90 (Fig. 1). It is notable that RNA B, which retains the C2507-G2582 base pair of this tertiary interaction, has a ninefold tighter $K_{app,RNA}$ than RNA C, which lacks these nucleotides. Because hairpin 92, nucleotides at the top of helix 90, and the 5′ and 3′ extensions of RNA A are all important for optimal binding of DbpA, it is possible that a compact structure similar to that observed in the ribosome may be relevant to DbpA binding.

The bound RNA influences ATP binding affinity

In a second set of experiments, an apparent ATP-binding constant ($K_{M,ATP}$) for the DbpA–RNA complex was determined from the rate of ATP hydrolysis as a function of ATP concentration. The results shown in Table 1 indicate that the value of $K_{M,ATP}$ is dependent upon the identity of the bound RNA. RNAs B–E, which lack the 5′ and 3′ extensions of cofactor A, have $K_{M,ATP}$ values that are four- to eightfold higher than RNA A. The effect of the activating RNA on ATP binding was further investigated via inhibition experiments with the nonhydrolyzable nucleotide analog AMP-PNP. In the presence of RNA A, the K_I for AMP-PNP is approximately 15-fold lower than with cofactor B (Table 2). The differential binding of AMP-PNP in the presence of two different RNAs suggests that nucleotide binding is influenced by the bound RNA, a result that is consistent with the coupled binding of RNA and ATP. Previous studies with the DEAD protein eIF-4A and the DNA helicase Rep have shown that the binding of ATP and nucleic acid are coupled. In each of these cases, coupled binding of the nucleic acid and nucleotide cofactor was proposed to be associated with enzyme conformational states in the reaction pathway (Lohman, 1993; Lorsch & Herschlag, 1998).

TABLE 2. RNA-specific AMP-PNP inhibition of DbpA.

RNA	$K_{I,AMP\text{-}PNP}$ (μM)	$K_{M,ATP}$ (μM)
A	25	120
B	440	510

The activity of 20 nM DbpA in the presence of saturating concentrations of cofactor A and 120 μM ATP, or saturating cofactor B and 510 μM ATP were assayed between 0 and 880 μM AMP-PNP in buffer A. The apparent competitive inhibition constant (K_I) was determined as described in the Materials and Methods.

Sequence requirements of RNA-dependent ATPase activity

RNAs D and E were used to determine the sequence requirements of DbpA's RNA-dependent ATPase activity. Both of these small RNAs consist of only two structural elements, hairpin 92 and a single-stranded extension, yet can fully stimulate the ATPase activity of DbpA when the RNA concentration is saturating. Eight variants of RNA D and four variants of RNA E were created; each introduces two to five changes in either hairpin 92 or the adjacent RNA extension (Fig. 2). Nondenaturing gels were used to confirm that none of the mutant RNAs aggregate or form alternate conformers under the conditions used in these assays. The 12 mutant RNAs were assayed for stimulation of ATPase activity in buffer B, which has a lower monovalent salt concentration than buffer A. The lower ionic strength buffer does not affect the ATPase activity, but increases the affinity of the RNA–protein complex, facilitating the characterization of RNAs that bind less well.

The results of these mutagenesis experiments are shown in Table 3 and can be summarized in a simple manner. Mutations in hairpin 92 greatly reduce the ability of the RNA to stimulate ATPase activity, whereas changes in the RNA extension have no effect. Thus the hairpin 92 sequence and an adjacent segment of RNA are required for the stimulation of ATPase activity. However, neither the sequence nor orientation (5′ versus 3′) of the RNA extension has an effect on the stimulation of ATPase activity.

Although hairpin 92 is clearly a recognition element for DbpA, the isolated hairpin does not stimulate ATPase activity. Moreover, a 14-fold excess of RNA I is required to halve the ATPase activity of DbpA and RNA D, present at its 100 nM $K_{app,RNA}$ (results not shown). The observation that hairpin 92 is neither an activator nor effective inhibitor of ATPase activity suggests that the single-stranded extensions of RNAs D and E are required both for high affinity RNA binding and for stimulation of ATP hydrolysis. As these extensions have no discernable sequence requirements, it is likely that they contribute to binding primarily through backbone contacts.

A model for the interaction of DbpA with 23S rRNA

The N-terminal 350 amino acids of DbpA are likely to have a structure similar to other DEAD proteins including eIF-4A and a related protein from *Methanococcus jannaschii* for which X-ray crystal structures have recently been solved (Caruthers et al., 2000; Story et al., 2001). These proteins each contain two parallel α-β

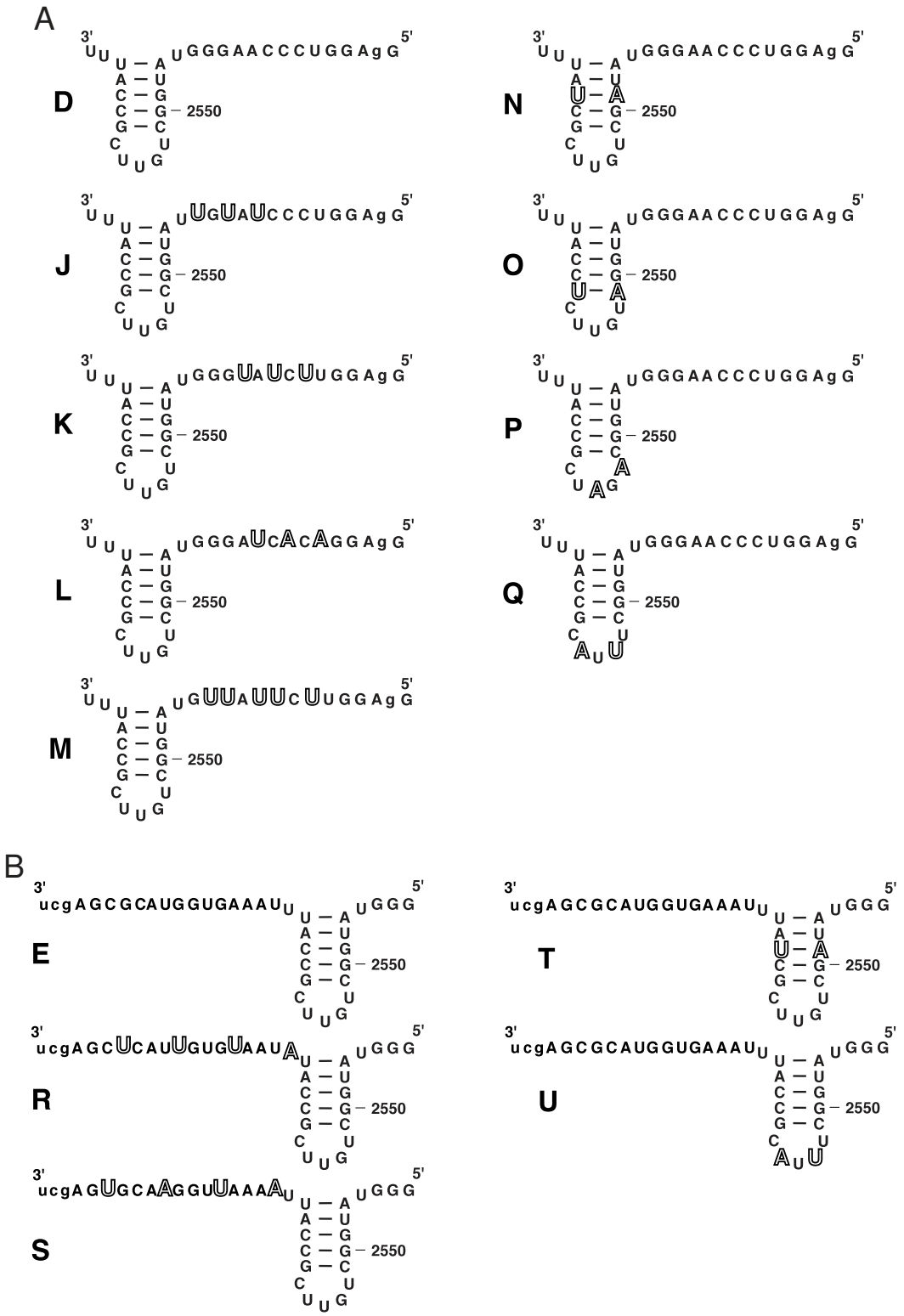

FIGURE 2. Mutants of RNA cofactors D (**A**) and E (**B**). Mutated nucleotides are shown in outlined text, and nucleotides that differ from 23S rRNA are shown in lowercase.

domains, an architecture similar to that observed in four other helicases (Korolev et al., 1997; Kim et al., 1998; Theis et al., 1999; Velankar et al., 1999). In most of these structures, the two domains are positioned opposite each other, separated by a deep interdomain cleft. Clustered at the narrow end of the cleft, where the two domains are connected, are several of the conserved amino acids responsible for ATP binding and

TABLE 3. Kinetic constants for site-directed mutants of RNAs D and E.

RNA	Region of mutation	k_{max} (min^{-1})	$K_{app,RNA}$ (nM)	$k_{max}/K_{app,RNA}$ (min^{-1} nM^{-1})	k_{cat} (min^{-1})	$K_{M,ATP}$ (μM)	$k_{cat}/K_{M,ATP}$ (min^{-1} μM^{-1})
2532–2563							
D	—	400	100	4	510	450	1.1
J	Single-stranded	460	145	3.2	470	260	1.8
K	Single-stranded	380	82	4.6	320	270	1.2
L	Single-stranded	410	140	2.9	330	370	0.89
M	Single-stranded	460	40	11.5	450	180	2.5
N	Stem	130	2250	0.058	—	—	0.058[b]
O	Stem	—	—	0.0085[a]	—	—	0.035[b]
P	Loop	—	—	0.060[a]	—	—	0.17[b]
Q	Loop	—	—	≤0.002[c]	—	—	ND
2543–2577							
E	—	360	200	1.9	—	—	ND
R	Single-stranded	340	700	0.49	—	—	ND
S	Single-stranded	270	900	0.30	—	—	ND
T	Stem	—	—	0.012[a]	—	—	ND
U	Loop	—	—	0.0028[a]	—	—	ND
2545–2563							
I	Hairpin alone	—	—	0.0023[a]	—	—	ND

Kinetic constants were determined in buffer B. The invariant substrate was held at saturating levels: 5 mM ATP, or RNA concentrations at least sixfold over K_{app} (3 μM RNA if $K_{app,RNA}$ could not be determined). DbpA was in the range of 10–50 nM, and was less than the lowest substrate concentration used.

[a] Derived from a linear plot of activity versus RNA concentration as described in Material and Methods.

[b] Estimated $k_{cat}/K_{M,ATP}$, as full RNA saturation could not be achieved.

[c] Estimated upper limit based on initial data.

hydrolysis. The wide end of the cleft contains conserved motifs involved in nucleic acid binding. Cocrystal structures of the PcrA, Rep, and HCV NS3 helicases with bound single-stranded oligonucleotides indicate the majority of contacts involve the nucleic acid backbone (Korolev et al., 1997; Kim et al., 1998; Velankar et al., 1999). Structural evidence suggests that binding of nucleic acid to the base of the interdomain cleft is linked to conformational changes in the ATP-binding site, which facilitate ATP hydrolysis (Soultanas et al., 1999; Velankar et al., 1999). Because the N-terminus of DbpA has sequence motifs similar to these helicases, it is likely that it shares a similar structure and has similar ATP and single-stranded nucleic acid binding capabilities.

Following the conserved sequence motifs present in all $DEx^D/_H$ proteins, DbpA has a carboxy-terminal domain of 70 amino acids that identifies it as a member of a subfamily of bacterial $DEx^D/_H$ proteins, including its homolog YxiN from *Bacillus subtilis* (Kossen & Uhlenbeck, 1999). A recent alignment of the C-terminal domains of 18 members of this subfamily identifies seven conserved basic residues, a conserved aromatic amino acid, and at least 17 conserved hydrophobic amino acids along its 70 amino acid length. The pattern of conserved amino acids in this domain and the demonstration that YxiN has a specificity for the same region of 23S rRNA led to a model in which the C-terminal domain of DbpA is responsible for sequence-specific RNA binding (Kossen & Uhlenbeck, 1999). The characterization of DbpA's RNA sequence specificity presented here makes it possible to refine this model. Two key components to the binding of RNA by DbpA were identified: an essential interaction with hairpin 92 that is sequence specific but does not activate the ATPase, and an interaction with an RNA extension 3′ or 5′ to hairpin 92 that is not sequence specific but is required for ATPase activity. Both these components contribute to the overall binding affinity so that neither the isolated hairpin nor the nonspecific RNA extension effectively bind (or activate) DbpA. The simplest way to reconcile these data is the model shown in Figure 3. The C-terminal domain of DbpA interacts with hairpin 92 in a sequence-specific manner whereas the adjacent RNA segment 5′ (or 3′) of it interacts with the N-terminal domains and activates the ATPase in a sequence-nonspecific manner similar to other helicases. In this model, the C-terminal domain confers specificity for the RNA target site as well as increasing the overall affinity of the RNA–protein interaction so that the N-terminal domains can access the adjacent RNA extension that stimulates the ATPase. It is noteworthy that the affinity of DbpA for its RNA target is considerably tighter than the minimal DEAD protein eIF-4A for single-stranded oligonucleotides (Lorsch & Herschlag, 1998), presumably because the C-terminal domain contributes to the overall affinity.

The unique sequence specificity of DbpA for RNA can therefore be understood by the fact that it acquired a sequence-specific RNA-binding domain to direct it to its 23S rRNA target. Because other $DEx^D/_H$ proteins appear to acquire their target specificity by association with a ribonucleoprotein particle (Roy et al., 1995; Wang

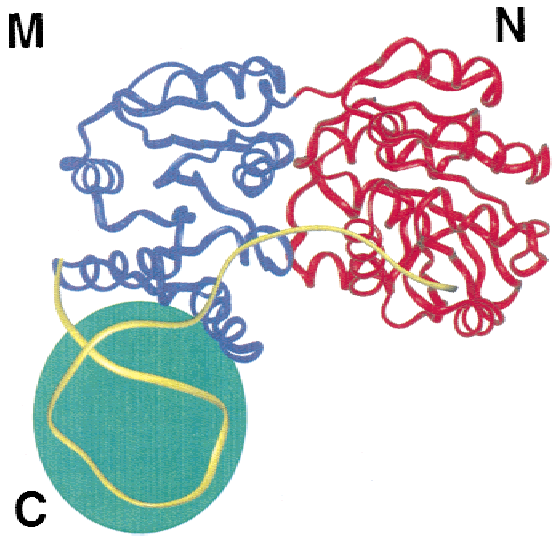

FIGURE 3. Model for the interaction of DbpA with RNA D. The first two domains of DbpA (N and M) contain sequence motifs shared among all helicases. Homologous domains were rendered from the structure of a DEAD protein from *M. jannaschii* (Story et al., 2001), and are shown in red and blue. Conserved sequence motifs involved in ATP binding and hydrolysis are clustered near the top of the cleft separating domains N and M, and residues implicated in RNA binding are located across their base. The unique carboxy-terminus of DbpA (C, green), which is associated with RNA sequence specificity, is shown in a position similar to the third domain in a DNA cocrystal structure of the HCV NS3 helicase (Kim et al., 1998). RNA D (yellow) was modeled using Weblab viewer. The model depicted here predicts that the unique carboxy-terminal domain of DbpA interacts with hairpin 92 in a sequence-specific manner, whereas additional nonspecific interactions are formed between amino acids at the base of the conserved helicase domains and the RNA extension.

& Guthrie, 1998), why has DbpA developed a different strategy? The answer may lie in the unique nature of the RNA target. Hairpin 92, the major site of sequence-specific binding for DbpA, is a highly conserved structural element that lies at the heart of the peptidyl transferase center of the ribosome where it participates in binding the CCA terminus of tRNA in the ribosomal A site (Kim & Green, 1999). Based on the recently completed X-ray structure of the 50S subunit (Nissen et al., 2000), hairpin 92 is not close to any ribosomal protein. Thus, if the function of DbpA is to act on the ribosome or a preribosomal particle, it cannot be directed to its site by binding another protein, but instead must specifically bind RNA directly. It is, however, important to state that neither the function nor the physiological substrate of DbpA is yet known. Although hairpin 92 is accessible to tRNAs during translation, neither mature ribosomes nor 50S subunits strongly stimulate the ATPase activity of DbpA (Tsu & Uhlenbeck, 1998), making its function in translation less likely. A more likely role for DbpA is that it assists in forming the complex structure of the peptidyl transferase center during ribosome biogenesis. Therefore, the function of DbpA may be similar to one of the 16 $DEx^{D}/_{H}$ proteins which act at various steps in yeast ribosome biogenesis (de la Cruz et al., 1999; Colley et al., 2000).

MATERIALS AND METHODS

RNA cofactors

Subfragments of *E. coli* 23S rRNA were prepared by three different methods. Templates for transcription of RNAs A–C, E, F, and R–U (Figs. 1 and 2B) by T7 RNA polymerase were subcloned into pUC19. The resulting plasmids were digested with appropriate restriction enzymes, and the desired RNAs produced via run-off transcription. RNAs D, G, H, and J–Q (Figs. 1 and 2A) were prepared by T7 transcription from synthetic DNA templates (Milligan & Uhlenbeck, 1989). RNA I (Fig. 2A) was chemically synthesized and deprotected (Wincott et al., 1995).

Crude preparations of RNAs D, E, and I–U were gel purified. All other RNAs were purified by acid phenol-chloroform extraction, ethanol precipitation, and size exclusion chromatography. RNA concentrations assume $\epsilon_{260} = 8{,}600\ M^{-1}\ cm^{-1}\ nt^{-1}$. Prior to use, each RNA was refolded in either 50 mM HEPES-K, pH 7.5, 50 mM KCl (for assay in buffer A), or 50 mM HEPES-K, pH 7.5 (for assay in buffer B) by heating for 30 s at 100 °C, followed by 90 s at 65 °C. $MgCl_2$ was then added to a final concentration of 5 mM. The propensity of the RNAs to form alternate conformers was assessed using 6% native polyacrylamide gels (Fedor & Uhlenbeck, 1990). All RNAs used in this study were found to adopt a single predominant structure at the concentrations used.

Spectroscopic ATPase assay

DbpA was prepared as described (Tsu & Uhlenbeck, 1998). An enzymatically coupled spectroscopic assay was employed to monitor the ATPase activity of DbpA (Tsu & Uhlenbeck, 1998). Most experiments were carried out at 37 °C in the standard buffer A: 50 mM HEPES-K, pH 7.5, 50 mM KCl, 5 mM $MgCl_2$, 100 μM DTT, 200 μM NADH, 1 mM phospho(enol)pyruvate, 13 μg/mL lactate dehydrogenase, 23 μg/mL pyruvate kinase. Other experiments were performed in buffer B, which was identical to buffer A, except that KCl was omitted. ATP and AMP-PNP were added in equimolar complex with Mg^{2+} ($ATP{\bullet}Mg^{2+}$). Working concentrations of DbpA were in the range of 5–50 nM, and were less than the lowest substrate concentration used. In the absence of RNA, the ATPase activity of DbpA was 0.25 ATP min^{-1} (Tsu & Uhlenbeck, 1998). All kinetic experiments were performed in duplicate for six to eight data points and a buffer blank. Experimental error was generally 10% or less, and the variability between independent determinations was approximately 20%, reflecting differences in RNA and protein preparations. Initial rates and kinetic fits were analyzed using Kaleidagraph (Synergy software). k_{max}, $K_{app,RNA}$, k_{cat}, and $K_{M,ATP}$ were derived using the Michaelis–Menten equation, as described previously (Tsu & Uhlenbeck, 1998). If RNA saturation could not be achieved, the apparent second-order RNA-binding constant ($k_{max}/K_{app,RNA}$) was taken as the linear slope of a plot of ATPase activity versus RNA concentration. In the absence of RNA saturation, estimates of $k_{cat}/K_{M,ATP}$ were determined from activity plots at 3 μM RNA. Inhibition of ATPase activity as a function of AMP-PNP concentration was monitored at 20 nM DbpA, saturating RNA, with ATP present at its K_M. The apparent competitive inhibitor binding constant, K_I, of AMP-PNP versus ATP was determined using the equation:

$$a = 1 - \frac{[I]}{[I] + K_I\left(1 + \frac{[S]}{K_M}\right)},$$

where a is the fractional activity, $[I]$ is the concentration of AMP-PNP, and K_M is the apparent binding constant of the ATP substrate $[S]$ (Segel, 1993).

ACKNOWLEDGMENTS

The authors thank Camille Diges, Evelyn Jabri, Audra Kammerer, Fedor Karginov, and Kevin Polach for many stimulating discussions and comments in the preparation of this manuscript. We thank Randall Story for supplying plasmids for the transcription of RNAs B and C, and for providing structural coordinates prior to publication. This work was funded by National Institutes of Health Grants GM37552 and GM60268 to O.C.U. and by a postdoctoral fellowship from the Jane Coffin Childs Memorial Fund for Medical Research to C.A.T.

Received January 26, 2001; returned for revision February 23, 2001; revised manuscript received March 5, 2001

REFERENCES

Anderson JS, Parker R. 1996. RNA turnover: The helicase story unwinds. *Curr Biol 6*:780–782.

Ban N, Nissen P, Hansen J, Moore PB, Steitz TA. 2000. The complete atomic structure of the large ribosomal subunit at 2.4 Å resolution. *Science 289*:905–920.

Caruthers JM, Johnson ER, McKay DB. 2000. Crystal structure of yeast initiation factor 4A, a DEAD-box RNA helicase. *Proc Natl Acad Sci USA 97*:13080–13085.

Colley A, Beggs JD, Tollervey D, Lafontaine DL. 2000. Dhr1p, a putative DEAH-box RNA helicase, is associated with the box C+D snoRNP U3. *Mol Cell Biol 20*:7238–7246.

de la Cruz J, Kressler D, Linder P. 1999. Unwinding RNA in *Saccharomyces cerevisiae*: DEAD-box proteins and related families. *Trends Biochem Sci 24*:192–198.

Fedor MJ, Uhlenbeck OC. 1990. Substrate sequence effects on "hammerhead" RNA catalytic efficiency. *Proc Natl Acad Sci USA 87*:1668–1672.

Fuller-Pace F. 1994. RNA helicases: Modulators of RNA structure. *Trends Cell Biol 4*:271–274.

Hirling H, Scheffner M, Restle T, Stahl H. 1989. RNA helicase activity associated with the human p68 protein. *Nature 339*:562–564.

Jankowsky E, Gross CH, Shuman S, Pyle AM. 2000. The DExH protein NPH-II is a processive and directional motor for unwinding RNA. *Nature 403*:447–451.

Kim DF, Green R. 1999. Base-pairing between 23S rRNA and tRNA in the ribosomal A site. *Mol Cell 4*:859–864.

Kim JL, Morgenstern KA, Griffith JP, Dwyer MD, Thomson JA, Murcko MA, Lin C, Caron PR. 1998. Hepatitis C virus NS3 RNA helicase domain with a bound oligonucleotide: The crystal structure provides insights into the mode of unwinding. *Structure 6*:89–100.

Korolev S, Hsieh J, Gauss GH, Lohman TM, Waksman G. 1997. Major domain swiveling revealed by the crystal structures of complexes of *E. coli* Rep helicase bound to single-stranded DNA and ADP. *Cell 90*:635–647.

Korolev S, Yao N, Lohman TM, Weber PC, Waksman G. 1998. Comparisons between the structures of HCV and Rep helicases reveal structural similarities between SF1 and SF2 super-families of helicases. *Protein Sci 7*:605–610.

Kossen K, Uhlenbeck OC. 1999. Cloning and biochemical characterization of Bacillus subtilis YxiN, a DEAD protein specifically activated by 23S rRNA: Delineation of a novel sub-family of bacterial DEAD proteins. *Nucleic Acids Res 27*:3811–3820.

Laggerbauer B, Achsel T, Lührmann R. 1998. The human U5-2OOkD DEXH-box protein unwinds U4/U6 RNA duplices in vitro. *Proc Natl Acad Sci USA 95*:4188.

Leffers H, Kjems J, Ostergaard L, Larsen N, Garrett RA. 1987. Evolutionary relationships amongst archaebacteria. A comparative study of 23 S ribosomal RNAs of a sulphur-dependent extreme thermophile, an extreme halophile and a thermophilic methanogen. *J Mol Biol 195*:43–61.

Lohman TM. 1993. Helicase-catalyzed DNA unwinding. *J Biol Chem 268*:2269–2672.

Lorsch JR, Herschlag D. 1998. The DEAD box protein eIF4A. 1. A minimal kinetic and thermodynamic framework reveals coupled binding of RNA and nucleotide. *Biochemistry 37*:2180–2193.

Luking A, Stahl U, Schmidt U. 1998. The protein family of RNA helicases. *Crit Rev Biochem Mol Biol 33*:259–296.

Milligan JF, Uhlenbeck OC. 1989. Synthesis of small RNAs using T7 RNA polymerase. *Methods Enzymol 180*:51–62.

Nicol SM, Fuller-Pace FV. 1995. The "DEAD box" protein DbpA interacts specifically with the peptidyltransferase center in 23S rRNA. *Proc Natl Acad Sci USA 92*:11681–11685.

Nissen P, Hansen J, Ban N, Moore PB, Steitz TA. 2000. The structural basis of ribosome activity in peptide bond synthesis. *Science 289*:920–930.

Pause A, Sonenberg N. 1992. Mutational analysis of a DEAD box RNA helicase: The mammalian translation initiation factor eIF-4A. *EMBO J 11*:2643–2654.

Pause A, Sonenberg N. 1993. Helicases and RNA Unwinding in Translation. *Curr Opin Struct Biol 3*:953–959.

Preugschat F, Averett DR, Clarke BE, Porter DJT. 1996. A steady-state and pre-steady-state kinetic analysis of the NTPase activity associated with the hepatitis C virus NS3 helicase domain. *J Biol Chem 271*:24449–24457.

Pugh GE, Nicol SM, Fuller-Pace FV. 1999. Interaction of the *Escherichia coli* DEAD box protein DbpA with 23 S ribosomal RNA. *J Mol Biol 292*:771–778.

Rogers GW Jr, Richter NJ, Merrick WC. 1999. Biochemical and kinetic characterization of the RNA helicase activity of eukaryotic initiation factor 4A. *J Biol Chem 274*:12236–12244.

Roy J, Kim K, Maddock JR, Anthony JG, Woolford JL Jr. 1995. The final stages of spliceosome maturation require Spp2p that can interact with the DEAH box protein Prp2p and promote step 1 of splicing. *RNA 1*:375–390.

Schmid SR, Linder P. 1992. D-E-A-D protein family of putative RNA helicases. *Mol Microbiol 6*:283–291.

Segel I. 1993. *Enzyme kinetics*. New York: John Wiley & Sons, Inc.

Soultanas P, Dillingham MS, Velankar SS, Wigley DB. 1999. DNA binding mediates conformational changes and metal ion coordination in the active site of PcrA helicase. *J Mol Biol 290*:137–148.

Staley JP, Guthrie C. 1998. Mechanical devices of the spliceosome: Motors, clocks, springs, and things. *Cell 92*:315–326.

Story RM, Li H, Abelson JN. 2001. Crystal structure of a DEAD box protein from the hyperthermophile *Methanococcus jannaschii*. *Proc Natl Acad Sci USA 98*:1465–1470.

Theis K, Chen PJ, Skorvaga M, Van Houten B, Kisker C. 1999. Crystal structure of UvrB, a DNA helicase adapted for nucleotide excision repair. *EMBO J 18*:6899–6907.

Tsu CA, Uhlenbeck OC. 1998. Kinetic analysis of the RNA-dependent adenosinetriphosphatase activity of DbpA, an *Escherichia coli* DEAD protein specific for 23S ribosomal RNA. *Biochemistry 37*:16989–16996.

Velankar SS, Soultanas P, Dillingham MS, Subramanya HS, Wigley DB. 1999. Crystal structures of complexes of PcrA DNA helicase with a DNA substrate indicate an inchworm mechanism. *Cell 97*:75–84.

Wang Y, Guthrie C. 1998. PRP16, a DEAH-box RNA helicase, is recruited to the spliceosome primarily via its nonconserved N-terminal domain. *RNA 4*:1216–1229.

Wang Y, Wagner JD, Guthrie C. 1998. The DEAH-box splicing factor Prp16 unwinds RNA duplexes in vitro. *Curr Biol 8*:441–451.

Wassarman DA, Steitz JA. 1991. RNA splicing. Alive with DEAD proteins. *Nature 349*:463–464.

Wincott F, DiRenzo A, Shaffer C, Grimm S, Tracz D, Workman C, Sweedler D, Gonzalez C, Scaringe S, Usman N. 1995. Synthesis, deprotection, analysis and purification of RNA and ribozymes. *Nucleic Acids Res 23*:2677–2684.